Nuclear Physics A524 (1991) 306-320
North-Holland

DIRECT PROJECTILE BREAK-UP AND ITS RELATION TO THE ASTROPHYSICALLY RELEVANT FUSION REACTIONS*

C.A. BERTULANI

Instituto de Física, Universidade Federal do Rio de Janeiro, 21945 Rio de Janeiro, R.J., Brazil

M.S. HUSSEIN

Instituto de Física, Universidade de São Paulo, C.P. 20516, 01498 São Paulo, S.P., Brazil

Received 22 May 1990
(Revised 16 August 1990)

Abstract: The break-up into two pieces of weakly bound nuclei passing by the Coulomb field of a large-Z nucleus can provide useful information on the inverse fusion reactions which are important for the elemental formation in the stars. However, the nuclear interaction complicates considerably the extraction of such information. We make a study of the contributions of the Coulomb and nuclear interaction to the process, showing when the Coulomb break-up prevails and how a reliable separation of multipolarities can be done.

1. Introduction

The synthesis of elements in the Universe is characterized by radiative capture reactions at extremely low energies, well below the Coulomb barrier. The cross sections for these reactions are of relevance for determining the elemental abundances at various astrophysical sites. Experimentally, the reproduction and measurement of radiative capture cross sections in the laboratory is extremely difficult, due to their low value [1]). In view of this fact, it has been proposed [2]) the experimental study of the break-up of a projectile $a \to b + c$ into two fragments by the Coulomb field of a target nucleus, as a possible way to extract the radiative capture cross sections for the inverse process $b + c \to a$. This idea has been discussed by several authors [3-6]) and first experimental results along this line are encouraging [7-8]).

Some criticisms to this experimental approach has been raised [5,9]). One of the main problems is the contribution of the nuclear interaction to the break-up process which complicates the extraction of the photodisintegration cross sections. This could be avoided in subbarrier collisions, where the nuclear interaction is unimportant. However, at these energies the break-up cross sections are very small and hardly provide any advantage over the direct measurements of the astrophysical reactions in the laboratory. At high energies the break-up cross sections [5]) are large, but one has to be able to separate the nuclear and the Coulomb contribution to the process. Previous studies [2,4]) have shown that the ideal situation is attained in collisions around 100 MeV/nucleon. Also, the break-up process may be resonant

* Supported in part by the CNPq and FAPESP.

(sequential), in which the projectile is excited to resonant states above the break-up threshold, or direct to the free continuum states. The sequential break-up is expected to be important for fragments with approximate equal "charge-to-mass" ratio, like in $^6\mathrm{Li} \to \alpha + \mathrm{d}$. The distinctive features of direct and sequential break-up of ^{6}Li projectiles has been investigated in ref. [6]), where support to this statement is found. As pointed out by those authors, while sequential break-up can be well described, such as Coulomb excitation to bound states which live longer than the collision, the direct break-up involves energy dependent transition matrix elements into the continuum of the fragment states. These continuum states are, moreover, distorted by the Coulomb field of the target. Nonetheless, for projectile energies above some tens of MeV per nucleon the Coulomb distortion on the final states will be small. At such energies it is also expected that the direct break-up will be dominant, especially at very forward angles [5]).

Only a few multipolarities contribute to the radiative capture cross sections, due to selection rules. For example, the fusion reaction $\alpha + {}^{12}\mathrm{C} \to {}^{16}\mathrm{O} + \gamma$ is dominated by E1 and E2 matrix elements. The relative importance of each of these two multipolarities, as well as their interference, to the total cross section is still controversial in low energy reactions [10]). The advantage of the use of the Coulomb break-up to infer the (inverse) matrix elements is that each multipolarity depends differently on the projectile energy, as well as on the target charge and mass. Therefore, one could separate the different multipolarities by making small modifications in the experimental setups.

At high energies the elastic break-up will only occur in peripheral, or distant, collisions. Since there is almost no overlap of the nuclear matter of the nuclei, a reliable approximation can be made for the nuclear break-up mechanism in the framework of the soft spheres model of Karol [11]) whose inputs are the nuclear densities at the surface and the nucleon–nucleon transition amplitudes at forward angles. The Coulomb contribution to the break-up can be handled in the traditional fashion with a straightforward multipole expansion.

As examples of break-up reactions which are related to radiative capture processes of interest in astrophysics, we cite

$$^7\mathrm{Be} \to \alpha + {}^3\mathrm{He}\,, \tag{1a}$$

$$^{16}\mathrm{O} \to {}^{12}\mathrm{C} + \alpha\,, \tag{1b}$$

$$^6\mathrm{Li} \to \alpha + \mathrm{d}\,, \tag{1c}$$

$$^7\mathrm{Li} \to \alpha + \mathrm{t}\,. \tag{1d}$$

The threshold energies to ignite these reactions are, respectively, 1.58 MeV, 7.162 MeV, 1.47 MeV and 2.47 MeV. The reaction $^3\mathrm{He}(^4\mathrm{He}, \gamma)^7\mathrm{Be}$ affects the solar neutrino flux at solar temperatures and is closely related to the solar neutrino problem. The reaction $^{12}\mathrm{C}(\alpha, \gamma)^{16}\mathrm{O}$ is important for the stellar helium-burning in red giant stars and for the determination of the C/O ratio. The formation of ^{6}Li

and ^{7}Li is relevant for testing the standard Big Bang model and the nucleosynthesis in the early Universe. All these reactions are needed at very low center-of-mass energies, corresponding to the temperatures in the stars [2]).

By means of the detailed balance theorem the radiative capture reactions can be related to the photodisintegration reactions, which are favoured by the phase space except in the extreme case very close to the threshold. Furthermore, the copious source of virtual photons present in the Coulomb field of a large-Z nucleus offers a more promising way to study the photo-dissociation process.

As shown in ref. [2]) this encourages the experimental studies of Coulomb break-up of loosely bound nuclei incident on heavy targets to have access to the radiative capture cross sections of interest in astrophysics.

In this article we study the interplay of the nuclear and Coulomb intereaction in the elastic break-up process. Although some important ingredients of the problem, like final-state interactions between the fragments, "post-acceleration" effects [2]), etc., are not considered here, our results envisage the regions of phase-space where experimental efforts should be concentrated. In sect. 2 we develop a calculation of the matrix elements for the elastic break-up based on the "soft-spheres" model of Karol [11]). Since the nucleon-nucleon scattering amplitudes are used as input, it is necessary to include "in-medium" corrections, namely the Pauli-blocking effect. This is done by means of the "local density approximation". This allows us to obtain an effective optical potential appropriate for collisions at energies around 100 MeV/nucleon. After that we perform a multipole expansion of both Coulomb and nuclear potentials, what leads to a separation of the center-of-mass and intrinsic coordinates of the clusters. In sect. 3 we use model wave functions to deduce the center-of-mass scattering amplitudes and the amplitudes for the transition from the bound to the continuum states of the clusters. Closed-form expressions are obtained. Sect. 4 deals with the applications of the formalism developed in the previous sections. Some simple situations are chosen, for which good experimental strategies could be accomplished. Our conclusions are given in sect. 5.

2. Elastic break-up in eikonal approximation

We consider the reaction

$$a+A\rightarrow b+x+A\,, \tag{2.1}$$

where a is a cluster-like projectile which fragments into two pieces (b+x) when it hits a target A. The transition matrix element in DWBA is (see fig. 1)

$$T_{fi}=\langle X^{(-)}_{a,k_a}(\boldsymbol{R})\phi^{(-)}_{xb,f}(\boldsymbol{r})|[\,U_{xA}(\boldsymbol{r}_{xA})+U_{bA}(\boldsymbol{r}_{bA})-U_{aA}(\boldsymbol{R})]|X^{(+)}_{a,k_a}(\boldsymbol{R})\phi^{(+)}_{xb,i}(\boldsymbol{r})\rangle\,, \tag{2.2}$$

where the U's are optical potentials, ϕ_{xb} is the wavefunction of relative motion of x+b, and $X^{(+)}_a$ is the distorted wave for a. In the final state $X^{(-)}_a$ represents the distorted wave in the c.m. of x+b. In the way (2.2) is written, the matrix element of U_{aA} is zero because $\langle\phi^{(-)}_{xb,f}|\,\phi^{(+)}_{xb,i}\rangle=0$. All coordinates are referred to the lab system,

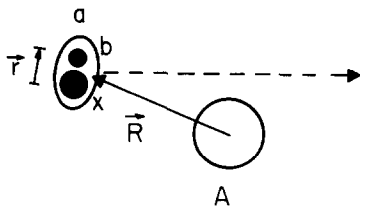

Fig. 1. A two-cluster nucleus is dissociated when hitting a heavy target in a peripheral collision. The coordinates used in the text are shown.

with the target as origin. The coordinates $\boldsymbol{r}_{xA}$ and $\boldsymbol{r}_{bA}$ are defined by

$$\boldsymbol{r}_{xA} = \boldsymbol{R} - \frac{m_b}{m_a}\boldsymbol{r}, \qquad \boldsymbol{r}_{bA} = \boldsymbol{R} + \frac{m_x}{m_a}\boldsymbol{r}. \tag{2.3}$$

For the nuclear optical potential, we use the Karol model [11]), which gives for example

$$U_{xA} = \langle t_{NN}(E)\rangle \pi^{3/2}\rho_A(0)\rho_x(0)\frac{a_x^3 a_A^3}{(a_x^2+a_A^2)^{3/2}}\exp\left[-r_{xA}^2/(a_x^2+a_A^2)\right] + \frac{Z_x Z_A}{r_{xA}} \tag{2.4}$$

where $\rho(r)$ is the nuclear density parametrized by $\rho(0)\,e^{-r^2/a_i^2}$, with adjusted $\rho(0)$ and a_i in order to reproduce the S-matrix for the elastic scattering in the WKB approximation, and $\langle t_{NN}(E)\rangle$ is a nuclear matter average of the nucleon-nucleon amplitude at $\Theta = 0$.

Assuming that the actual nuclear matter densities can be described by a Fermi distribution

$$\rho(r) = \frac{\rho_0}{1+\exp\left[(r-R)/d\right]}, \tag{2.5a}$$

where

$$R = 1.07A^{1/3}, \tag{2.5b}$$

$$d = t/44, \qquad t = 2.4\ \text{fm}, \qquad d = 0.54\ \text{fm}, \tag{2.5c}$$

$$\rho_0 = \frac{3A}{4\pi R^3}\left[1+(\pi^2 t^2/19.36R^2)\right]^{-1}, \tag{2.5d}$$

and comparing with the gaussian adjust $\rho(0)\,e^{-r^2/a_A^2}$ at $r = R_A$ and $r = R_A + \frac{1}{2}t$, one finds

$$\rho(0) = \tfrac{1}{2}\rho_0\, e^{R^2/a_A^2}, \tag{2.6a}$$

$$a_A^2 = \frac{4Rt+t^2}{4\ln 5} \cong \frac{Rt}{\ln 5}. \tag{2.6b}$$

The free nucleon-nucleon amplitude $t_{NN}(E)$ can be deduced from the experiment. It can be written as

$$t_{NN}(E) = -\frac{4\pi\hbar^2}{2\mu} f(\theta = 0°) = -i\frac{\hbar v}{2}\sigma_{NN}^{tot}[1 - i\alpha_{exp}(E)], \tag{2.7}$$

where σ_{NN}^{tot} is the total cross section for free nucleon-nucleon collisions, v is the relative velocity, μ is the reduced mass and

$$\alpha_{exp}(E) = \mathrm{Re}\,[f(\theta = 0°)]/\mathrm{Im}\,[f(\theta = 0°)] \tag{2.8}$$

is determined experimentally [12,13]). For σ_{NN}^{tot} we use an average over isospin in the form

$$\langle\sigma_{NN}^{eff}\rangle = \frac{1}{A_A A_a}[(Z_a Z_A + N_a N_A)\sigma_{pp}^{eff} + (Z_a N_A + Z_A N_a)\sigma_{pn}^{eff}]. \tag{2.9}$$

The same average of α_{exp} can be made in terms of α_{pp} and α_{pn}. To correct for the Pauli-blocking effects in nucleus-nucleus collisions we use the result [14])

$$\sigma_{NN}^{eff}(E) = P(E, k_{F_1}, k_{F_2})\sigma_{NN}^{free}(E), \tag{2.10}$$

where P is a reduction factor of the cross section for nucleon-nucleon collisions in the nuclear medium. In the local density approximation the Fermi momenta k_{F_1} and k_{F_2} are related to the local densities by $k_{F_i} = (\frac{3}{2}\pi^2\rho_i)^{1/3}$. Since the nuclear break-up happens at the surface, we use ρ_1 and ρ_2 calculated at $r = R_1$ and R_2, respectively, i.e., $\rho_1(r = R_1)$ and $\rho_2(r = R_2)$. In this approximation,

$$P(E, k_{F_1}, k_{F_2}) = \frac{1}{(\frac{4}{3}\pi k_{F_1}^3)(\frac{4}{3}\pi k_{F_2}^3)}\int \mathrm{d}^3k_1\,\mathrm{d}^3k_2\,\Omega(\boldsymbol{k}, \boldsymbol{k}_1, \boldsymbol{k}_2)\frac{2q}{k}\frac{\sigma_{NN}^{free}(q)}{\sigma_{NN}^{free}(k)}, \tag{2.11}$$

where $\boldsymbol{k}_1$ and $\boldsymbol{k}_2$ are the momenta of the nucleons, k is their relative momentum and $2q = |\boldsymbol{k}_1 - \boldsymbol{k}_2 + \boldsymbol{k}|$. The function $\Omega(\boldsymbol{k}, \boldsymbol{k}_1, \boldsymbol{k}_2)$ is obtained analytically under the assumption of energy and momentum conservation of the pair and that they cannot scatter into the (filled) local Fermi spheres of radii k_{F_1} and k_{F_2}. Due to the cylindrical symmetry in the momentum space distribution, eq. (2.11) can be reduced to a fivefold integration [14]). In fig. 2 we present the results of a numerical calculation for P, as a function of the variables $\xi = k/k_{F>}$ and $\eta = k_{F<}/k_{F>}$, where $k_{F>}$ ($k_{F<}$) is the larger (smaller) of k_{F_1} and k_{F_2}. For simplicity we use $\sigma_{NN}^{free} = \frac{1}{2}(\sigma_{pp} + \sigma_{np})$. We observe that there will be an appreciable reduction of the free nucleon-nucleon cross section up to $k/k_{F>} \simeq 4$ due to the reduction of the available phase space for scattering. This means that Pauli blocking influences the nucleon-nucleon cross section for energies of relative motion up to 17 times the Fermi energy, if $k_{F>} = 1.35\ \mathrm{fm}^{-1}$. As an example, for $^{16}O + ^{208}Pb$ at 100 MeV/nucleon, the averaged nucleon-nucleon cross section in the surface region is reduced by a factor 0.65 as compared to the free nucleon-nucleon cross section. In our calculation, $\langle t_{NN}(E)\rangle$, as it appears in (2.4), includes the medium effect in the way described above.

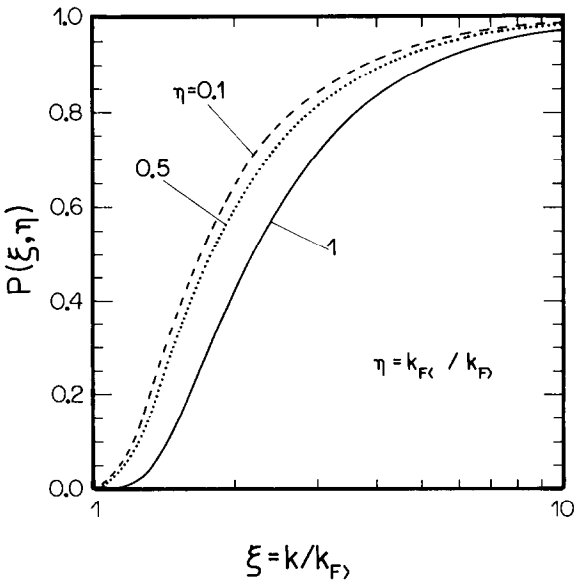

Fig. 2. Reduction factor for the nucleon-nucleon cross section corrected for medium (Pauli) effects. k is the nucleon-nucleon relative momentum, and $k_{F<}$ ($k_{F>}$) is the smaller (larger) of the local Fermi momentum at a given point of the overlapping nucleus.

As a result of the parametrization of the optical potentials in the form (2.4) we obtain that

$$U_{xA}+U_{bA}-U_{aA}\simeq U_{aA}^{N}(R)\left\{\exp\left\{-\left[\left(\frac{m_b}{m_a}\right)^2 r^2+2\frac{m_b}{m_a}\boldsymbol{r}\cdot\boldsymbol{R}\right]\Big/a^2\right\}\right.$$
$$\left.+\exp\left\{-\left[\left(\frac{m_x}{m_a}\right)^2 r^2-2\frac{m_x}{m_a}\boldsymbol{r}\cdot\boldsymbol{R}\right]\Big/a^2\right\}-1\right\}+Z_A e^2\left\{\frac{Z_b}{r_b}+\frac{Z_x}{r_x}-\frac{Z_a}{R}\right\}$$
$$=V^{N}(\boldsymbol{r},\boldsymbol{R})+V^{C}(\boldsymbol{r},\boldsymbol{R}), \tag{2.12}$$

where $a^2\simeq a_a^2+a_A^2\simeq a_b^2+a_A^2\simeq a_x^2+a_A^2$. Now a multipole expansion can be carried out, both for the nuclear as for the Coulomb part, resulting in

$$V^{N}(\boldsymbol{r},\boldsymbol{R})=4\pi U_{aA}^{N}(R)\left\{\sum_{L,M}(i)^L Y_{LM}^{*}(\hat{\boldsymbol{R}})\,Y_{LM}(\hat{\boldsymbol{r}})\right.$$
$$\times\left[\exp\left(-\left[\frac{m_b r}{m_a a}\right]^2\right)j_L\left(i2\frac{m_b}{m_a}\frac{rR}{a^2}\right)\right.$$
$$\left.\left.+(-1)^L\exp\left(-\left[\frac{m_x r}{m_a a}\right]^2\right)j_L\left(i2\frac{m_x}{m_a}\frac{Rr}{a^2}\right)\right]-1\right\}, \tag{2.13}$$

$$V^{\mathrm{C}}(\boldsymbol{r},\boldsymbol{R}) = 4\pi Z_{\mathrm{A}}\,\mathrm{e}^2 \sum_{L,M}\left[Z_{\mathrm{b}}\left(-\frac{m_{\mathrm{x}}}{m_{\mathrm{a}}}\right)^{L} + Z_{\mathrm{x}}\left(\frac{m_{\mathrm{b}}}{m_{\mathrm{a}}}\right)^{L}\right]$$
$$\times (2L+1)^{-1}\frac{r^L}{R^{L+1}}\,Y^*_{LM}(\hat{\boldsymbol{R}})\,Y_{LM}(\hat{\boldsymbol{r}})\,. \tag{2.14}$$

Since the nuclear break-up occurs near the surface, we put R inside the argument of j_L equal to $R_{\mathrm{T}} = R_{\mathrm{a}} + R_{\mathrm{A}}$, thus Rr/a^2 is replaced by $R_{\mathrm{T}}r/a^2$. With this approximation the matrix element $\langle X^{(-)}_{\mathrm{a,f}}(\boldsymbol{R})\phi^{(-)}_{\mathrm{xb,f}}(\boldsymbol{r})|\,V^{N}(\boldsymbol{r},\boldsymbol{R})|X^{(+)}_{\mathrm{a,i}}\phi^{(+)}_{\mathrm{xb,i}}\rangle$ factorizes and becomes

$$T^{\mathrm{N}}_{\mathrm{fi}} = 4\pi \sum_{L,M}\langle X^{(-)}_{\mathrm{a,f}}(\boldsymbol{R})|\,Y^*_{LM}(\hat{\boldsymbol{R}})\,U^{\mathrm{N}}_{\mathrm{aA}}(R)|X^{(+)}_{\mathrm{a,i}}(\boldsymbol{R})\rangle$$
$$\times \sum_{j=\mathrm{x,b}}\langle\phi^{(-)}_{\mathrm{xb,f}}(\boldsymbol{r})|v^{\mathrm{N}}_{j,L}(r)\,Y_{LM}(\hat{\boldsymbol{r}})|\phi^{(+)}_{\mathrm{xb,i}}(\hat{\boldsymbol{r}})\rangle$$
$$= \sum_{LM}(T^{\mathrm{N}}_{\mathrm{el}})_{LM}(T^{\mathrm{N}}_{\mathrm{exc}})_{LM}\,, \tag{2.15}$$

where

$$v^{\mathrm{N}}_{j,L}(r) = (-1)^{l_j}\exp\left[-\left(\frac{m_j r}{m_{\mathrm{a}}a}\right)^2\right] j_L\left(i2\,\frac{m_j}{m_{\mathrm{a}}}\,\frac{rR_{\mathrm{T}}}{a^2}\right) \tag{2.16}$$

with $l_j = L$ for $j = x$, and $l_j = 0$ for $j = b$. In (2.15), $T^{\mathrm{N}}_{\mathrm{el}}$ is the elastic factor of c.m. scattering of the projectile by the nuclear field and $T^{\mathrm{N}}_{\mathrm{exc}}$ is the excitation factor.

The Coulomb amplitude also factorizes into an elastic and an excitation factor, where

$$T^{\mathrm{C}}_{\mathrm{fi}} = \sum_{LM}(T^{\mathrm{C}}_{\mathrm{el}})_{LM}(T^{\mathrm{C}}_{\mathrm{exc}})_{LM} \tag{2.17}$$

with

$$(T^{\mathrm{C}}_{\mathrm{el}})_{LM} = 4\pi Z_{\mathrm{A}}e^2 \sum_{LM}\frac{1}{2L+1}\langle X^{(-)}_{\mathrm{a,f}}(\boldsymbol{R})|\,\frac{Y^*_{LM}(\hat{\boldsymbol{R}})}{R^{L+1}}\,|X^{(+)}_{\mathrm{a,i}}(\boldsymbol{R})\rangle\,, \tag{2.18}$$

$$(T^{\mathrm{C}}_{\mathrm{exc}})_{LM} = \sum_{LM}\left[Z_{\mathrm{b}}\left(-\frac{m_{\mathrm{x}}}{m_{\mathrm{a}}}\right)^{L} + Z_{\mathrm{x}}\left(\frac{m_{\mathrm{b}}}{m_{\mathrm{a}}}\right)^{L}\right]\langle\phi^{(-)}_{\mathrm{xb,f}}(\boldsymbol{r})|r^L Y_{LM}(\hat{\boldsymbol{r}})|\phi_{\mathrm{xb,i}}(\hat{\boldsymbol{r}})\rangle\,. \tag{2.19}$$

It is just the matrix elements in (2.19) which are of interest in nuclear astrophysics. In order to extract information on these matrix elements one has to be able to perform an accurate measurement of the break-up differential cross sections. When the spin orientation is not specified, the break-up cross sections when the center-of-mass wave vector of the fragments lies between $\boldsymbol{k}_{\mathrm{f}}$ and $\boldsymbol{k}_{\mathrm{f}} + \mathrm{d}\boldsymbol{k}_{\mathrm{f}}$, and the relative motion wave vector lies between $\boldsymbol{q}$ and $\boldsymbol{q} + \mathrm{d}\boldsymbol{q}$, is given by

$$\mathrm{d}\sigma = \frac{2\pi}{v}|T_{\mathrm{fi}}|^2\,\frac{\mathrm{d}^3k_{\mathrm{f}}\,\mathrm{d}^3q}{(2\pi)^6}\,\delta(E_{\mathrm{i}} - E_{\mathrm{f}})$$
$$= \frac{\mu k_{\mathrm{f}}\mu_{\mathrm{bx}}q}{(2\pi)^5\hbar^5 v}\left|\sum_{LM}\{T^{\mathrm{N}}_{LM} + T^{\mathrm{C}}_{LM}\}\right|^2 \mathrm{d}\Omega_{\mathrm{f}}\,\mathrm{d}\Omega_{\mathrm{q}}\,\mathrm{d}\varepsilon_{\mathrm{bx}}\,, \tag{2.20}$$

where $v(E)$ is the velocity (energy) of the projectile,

$$\boldsymbol{k}_f = \boldsymbol{k}_b + \boldsymbol{k}_x\,, \qquad \boldsymbol{q} = \frac{m_b}{m_a}\boldsymbol{k}_x - \frac{m_x}{m_a}\boldsymbol{k}_b\,, \tag{2.21}$$

and μ (μ_{bx}) is the reduced mass of the system a+A(b+x). The relative kinetic energy of the fragments after the break-up is $\varepsilon_{bx} = \hbar^2 q^2/2\mu_{bx}$. Using the energy and momentum conservation laws we can also rewrite (2.20) as

$$d\sigma = \frac{1}{\hbar^3 v}\frac{m_x k_x}{(2\pi)^5}\left|\sum_{LM}\{T^N_{LM} + T^C_{LM}\}\right|^2 d\Omega_x\, d^3k_b\,. \tag{2.22}$$

A theoretical calculation of the differential and total cross section from (2.20) or (2.22) is far from trivial and involves a large set of numerical integrations to determine the matrix elements T_{LM}. However, by using appropriate scattering wave functions some analytical results may be carried up to a point where numerical calculations are feasible. This is done in the next section. But, already at this point, some simple conclusions can be done in terms of the form of the matrix elments T_{LM}. First, the amplitude T_{LM} decrease with increasing multipolarity L, exponentially (nuclear case), or as a power of $R_a/R_T = R_a/(R_a+R_A)$ (Coulomb case). Therefore, only some few multipolarities need to be considered. We only account for the first two multipolarities, $L=1$ and $L=2$. Secondly, depending on the masses, or charge-to-mass ratio of the fragments, the contribution of the first multipolarity may be identically zero. The $L=1$ multipolarity corresponds to the homogeneous part of the field. If the masses of fragments are equal ($m_x = m_b$), from (2.15) and (2.16) one observes that the $L=1$ nuclear component is null. This happens because the homogeneous part of the nuclear force acts equally on both fragments and does not transfer a net relative momentum to them. Therefore, only the tidal ($L=2$) component of the field is effective in dissociating them. In the case of the Coulomb field the same happens for equal charge-to-mass ratio fragments, i.e., for $Z_x/m_x = Z_b/m_b$, because although the Coulomb force is proportional to the charge of each fragment, the resulting acceleration is proportional to the inverse of their masses. This is a well known result in bremmstrahlung of heavy-ion collisions which vanishes for equal charge-to-mass ratio partners.

3. Computation of the matrix elements

The center-of-mass wavefunctions $\chi^{(+)}_{a,i}$ and $\chi^{(-)}_{a,f}$ which enter into the matrix elements of eqs. (2.15) and (2.18) are evaluated within the eikonal approximations, as done in refs. [16,17]) for the inclusive break-up cross section:

$$\chi^{(+)}_{a,i}(\boldsymbol{R}) = e^{i\boldsymbol{k}_i\cdot\boldsymbol{R}}\exp\left\{-\frac{ik}{2E}\int_{-\infty}^{z} U_{aA}(z', b)\, dz' + i\phi_c(b)\right\}, \tag{3.1a}$$

$$\chi^{(-)^*}_{\mathrm{a,f}}(\boldsymbol{R}) = \mathrm{e}^{-i\boldsymbol{k}_\mathrm{f}\cdot\boldsymbol{R}} \exp\left\{-\frac{ik}{2E}\int_z^\infty U_{\mathrm{aA}}(z', b)\,\mathrm{d}z' + i\phi_\mathrm{c}(b)\right\}, \tag{3.1b}$$

where $\phi_\mathrm{c}(b) = Z_\mathrm{a}[Z_\mathrm{A}\alpha/(v/c)]\ln(kb)$ is the Coulomb phase, and $\alpha = 1/137$.

The excitation matrix elements for the transition $\phi_{\mathrm{xb,i}} \to \phi_{\mathrm{xb,f}}$ are just those that one is interested in astrophysical reactions. We shall use simplified model wavefunctions for this transition in order to obtain the general properties of the elastic break-up differential cross sections.

In the case of a δ-potential corresponding to the assumption of zero-range nuclear forces between the clusters in the projectile, we may use the following wavefunctions

$$\phi^{(+)}_{\mathrm{xb,i}} = \sqrt{\frac{\eta}{2\pi}}\,\frac{\mathrm{e}^{-\eta r}}{r}, \tag{3.2a}$$

$$\phi^{(-)}_{\mathrm{xb,f}} = \mathrm{e}^{-i\boldsymbol{q}\cdot\boldsymbol{r}} + \frac{1}{\eta - iq}\,\frac{\mathrm{e}^{iqr}}{r}, \tag{3.2b}$$

with $\boldsymbol{q}$ given by (2.21), and $\eta = (2\mu_{\mathrm{bx}}\varepsilon/\hbar^2)^{1/2}$ is determined by the separation energy, ε, of the clusters b+x.

Inserting (3.1) and (3.2) into the matrix elements (2.15), (2.18) and (2.19), one obtains after some approximations,

$$\begin{aligned}(T^N_{\mathrm{el}})_{LM} &= \langle\chi^{(-)}_{\mathrm{a,f}}(\boldsymbol{R})|\,Y^*_{LM}(\hat{\boldsymbol{R}})\,U^{\mathrm{N}}_{\mathrm{aA}}(R)|\chi^{(+)}_{\mathrm{a,i}}(\boldsymbol{R})\rangle \\ &= -2\pi C\beta_{LM}\,\mathrm{e}^{-Q_\ell^2 a^2/4} F_M(Q_\mathrm{t}),\end{aligned} \tag{3.3a}$$

where

$$C = \pi^2\langle t_{\mathrm{NN}}(E)\rangle\rho_\mathrm{A}(0)\rho_\mathrm{a}(0)\,\frac{a_\mathrm{a}^3 a_\mathrm{A}^3}{a^2}, \tag{3.3b}$$

$$\beta_{LM} = i^M\begin{cases}\sqrt{\dfrac{2L+1}{4\pi}}\,\dfrac{\sqrt{(L-M)!(L+M)!}}{(L-M)!!(L+M)!!}\,(-1)^{(L+M)/2} & L+M = \text{even} \\ 0 & L+M = \text{odd}.\end{cases} \tag{3.3c}$$

and

$$F_M(Q_\mathrm{t}) = \int_0^\infty b\,\mathrm{d}b\,J_M(Q_\mathrm{t}b)\,\mathrm{e}^{-b^2/a^2}\exp\left\{iC\frac{k}{E}\,\mathrm{e}^{-b^2/a^2} + 2i\phi_\mathrm{c}(b)\right\}. \tag{3.3d}$$

In the above expressions Q_ℓ and Q_t are the components of $\boldsymbol{Q}$ parallel and perpendicular to the z-axis, respectively; and $J_M(x)$ is the Bessel function of first kind. The integral (3.3d) has to be performed numerically and it governs the amount of momentum transferred.

The nuclear excitation matrix element is, accordingly

$$\begin{aligned}(T^{\mathrm{N}}_{\mathrm{exc}})_{LM} &= \sum_{j=\mathrm{x,b}}\langle\phi^{(-)}_{\mathrm{xb,f}}(\boldsymbol{r})|\,V^{\mathrm{N}}_{j,L}(r)\,Y_{LM}(\hat{\boldsymbol{r}})|\phi^{(+)}_{\mathrm{xb,i}}(\boldsymbol{r})\rangle \\ &= \sqrt{8\pi\eta}\;i^L Y_{LM}(\hat{\boldsymbol{q}})\{G_L(m_\mathrm{x}) + (-1)^L G_L(m_\mathrm{b})\},\end{aligned} \tag{3.4a}$$

where

$$G_L(m_j)=\int_0^\infty \mathrm{d}r\, r\, \mathrm{e}^{-\eta r} j_L(qr) j_L\left(2i\frac{m_j}{m_a}\frac{R_T r}{a^2}\right)\mathrm{e}^{-(m_j r/m_a a)^2}. \tag{3.4b}$$

The Coulomb amplitudes for the center-of-mass scattering are found to be

$$(T_{\mathrm{el}}^{\mathrm{C}})_{LM}=(4\pi)^2 Z_A\,\mathrm{e}^2\frac{\beta_{LM}}{(2L+1)(L-1)!!}Q_\ell^{L/2}H_{LM}(\boldsymbol{Q}), \tag{3.5a}$$

where

$$H_{LM}(\boldsymbol{Q})=\int_0^\infty b\,\mathrm{d}b\,J_M(Q_t b)\frac{\mathrm{e}^{-b^2/a^2}}{b^{L/2}}K_{L/2}(Q_\ell b)\exp\{iC\,\mathrm{e}^{-b^2/a^2}+2i\phi_C(b)\} \tag{3.5b}$$

with $K_\nu(x)$ equal to the modified Bessel function of first kind.

The Coulomb excitation amplitudes will be

$$(T_{\mathrm{exc}}^{\mathrm{C}})_{LM}=4\pi i^L Y_{LM}(\hat{\boldsymbol{q}})\left[Z_b\left(-\frac{m_x}{m_a}\right)^L+Z_x\left(\frac{m_b}{m_a}\right)^L\right]\frac{L!(2q)^L}{(\eta^2+q^2)^{L+1}}. \tag{3.6}$$

4. Applications and discussions

As an application of the formalism developed in the last two sections we take the reaction

$$^7\mathrm{Li}+{}^{208}\mathrm{Pb}\rightarrow\alpha+\mathrm{t}+{}^{208}\mathrm{Pb} \tag{4.1}$$

at 100 MeV per nucleon.

In fig. 3 we show the contour plots of the differential cross section $\mathrm{d}^2\sigma/\mathrm{d}k_\perp^\alpha\,\mathrm{d}k_\perp^{\mathrm{t}}$, where $k_\perp^j$ is the (final) transverse momentum of the respective cluster j. This quantity is especially useful since it can be measured experimentally without much difficulty.

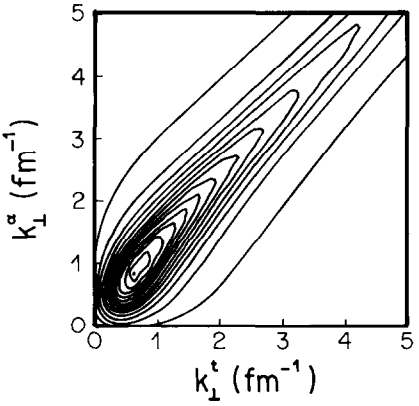

Fig. 3. Contour plots of the double-differential cross section (in arbitrary units) $\mathrm{d}^2\sigma/\mathrm{d}k_\perp^\alpha\,\mathrm{d}k_\perp^{\mathrm{t}}$ of tritium and alphas as a function of their transverse momentum in the lab system. They originate from the break-up of 100 MeV/nucleon ^{7}Li projectiles incident on ^{208}Pb.

It can be calculated from (2.22) by using $d\Omega_x \cong 2\pi k_\perp^x \, dk_\perp^x / k_x^2$, which is a good approximation for fastly moving particles.

One observes from this figure that there is a ridge in the cross section for $k_\perp^\alpha \simeq k_\perp^t$. Such feature is also observed for other break-up reactions and is peculiar to the peripheral processes [15]). The distribution has a maximum for transverse momentum equal to 0.7 fm^{-1}, which corresponds to a transverse energy of the fragments of order of 2.5 MeV. That is, the peak in transverse energy of the fragments is approximately of the same magnitude as the binding energy of the clusters. Such feature is also common to the peripheral dissociation of loosely bound particles [18]).

In fig. 4 we show $d\sigma/d\Omega_{c.m.}$ as a function of $\theta_{c.m.}$, for the same reaction (4.1), where $\theta_{c.m.}$ is the scattering angle of the center-of-mass of the clusters, as seen in the laboratory. We show separately the Coulomb, nuclear contributions and the interference between the two. Except for the very forward scattering angles, the Coulomb contribution prevails over the nuclear one. Interference is negative and two orders of magnitude smaller than the Coulomb dissociation, and may be neglected. The $L = 1$ terms in Coulomb and nuclear dissociation accounts almost entirely of the calculated cross sections. In this particular case, one observes that by selecting the angular interval between 1° and 3° one obtains the Coulomb contribution to the dissociation with only a 10% influence by the nuclear interaction.

In table 1 we show the contributions from each multipolarity to $d\sigma/d\Omega_{c.m.}$ for the dissociation of ^{7}Be, ^{7}Li, ^{16}O and ^{6}Li projectiles incident on ^{208}Pb at

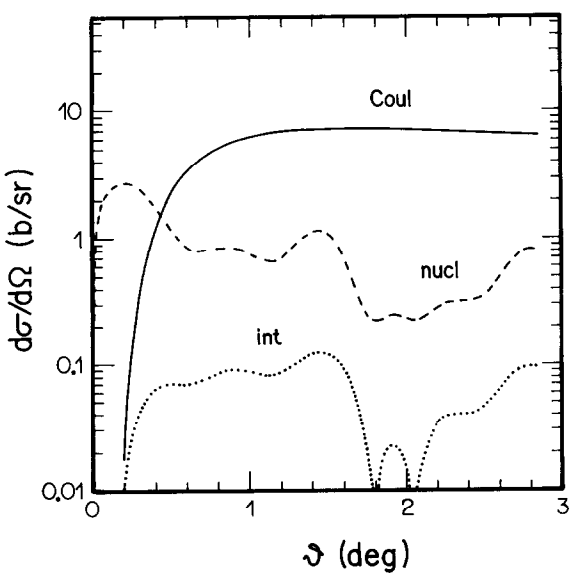

Fig. 4. Elastic differential cross section for the dissociation of ^{7}Li at 100 MeV/nucleon incident on ^{208}Pb, in the lab system. The Coulomb (solid curve), nuclear (dashed) and Coulomb-nuclear interference contributions to the break-up are shown separately.

TABLE 1

Differential cross section, $d\sigma/d\Omega$, in mb/sr, for the elastic break-up at $\theta_{lab} = 3°$ of several loosely bound nuclei incident or ^{208}Pb targets with 100 MeV/nucleon. The contribution of several Coulomb and nuclear multipolarities are displayed separately

	$L=1$		$L=2$		$L=3$	
	C	N	C	N	C	N
^{7}Be	122	45	31	22	4.7	0.3
^{16}O	0	84	52	48	2.9	3.1
^{7}Li	501	41	29	24	2.4	0.2
^{6}Li	0	23	18	15	1.5	2.0

100 MeV/nucleon, and for $\theta_{c.m.} = 3°$. We observe that, in those cases where the masses (charge-to-mass ratios) of the fragments are equal, or nearly equal, the nuclear (Coulomb) $L=1$ contribution to the cross section are drastically reduced. This occurs due to the selection rules for the dissociation amplitudes, as discussed in sect. 2. The final-state interactions between the fragments may modify such results, and are not considered here. But, a more exact treatment of the dissociation process should not destruct completely the fingerprints of these effects.

In fig. 5 we plot the differential cross section $d\sigma/d\varepsilon$ for the same reaction, as a function of the relative kinetic energy ε in the final state of fragments. One observes

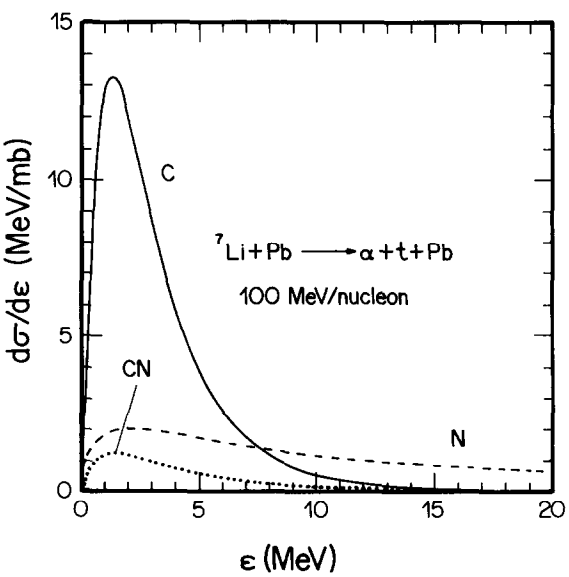

Fig. 5. Relative energy distribution of the fragments originated from the dissociation of ^{7}Li incident on ^{208}Pb at 100 MeV/nucleon. The solid and dashed curves give the Coulomb and nuclear contributions to the cross section, respectively.

that the Coulomb interaction favours the break-up into low relative kinetic energies, while the nuclear interaction develops a long tail for the kinetic energy distribution. Also shown is the Coulomb–nuclear interference, which is negative. Again one sees that the peak on the relative kinetic energy occurs for kinetic energy of order of the binding energy of the clusters.

In fig. 6 we present the triple-differential cross section $d^3\sigma/d\Omega_\alpha\, d\Omega_t\, dE_\alpha$ for the emission of α-particles at 3° and tritium at 1° in the lab system, as a function of the kinetic energies of the α-particles. The Coulomb (solid curve) and nuclear (dashed curve) are shown separately. Again we see that the Coulomb dissociation prevails over the nuclear one in a narrow energy region. The width of the Coulomb peak is appreciably smaller than the width of the nuclear peak, similarly to what was shown for the relative energy distribution of fig. 5.

From what was shown in figs. 2–6, it seems clear that, only in the very forward angular regions, and for a very narrow energy interval, the Coulomb contribution to the dissociation process can be reasonably disentangled from the nuclear contribution. This means that very dedicated experimental efforts have to be put in order to achieve this goal and relate the break-up experiments to the associated fusion reaction. Recent experiments on ^{6}Li and ^{7}Li break-up [19–21]) at 26 MeV/nucleon and 9 MeV/nucleon, respectively, have shown the feasibility of the method. However, as was suggested in ref. [2]), the ideal situation occurs for beam energies around 100 MeV/nucleon. At such energies it may be critical to determine the relative energy

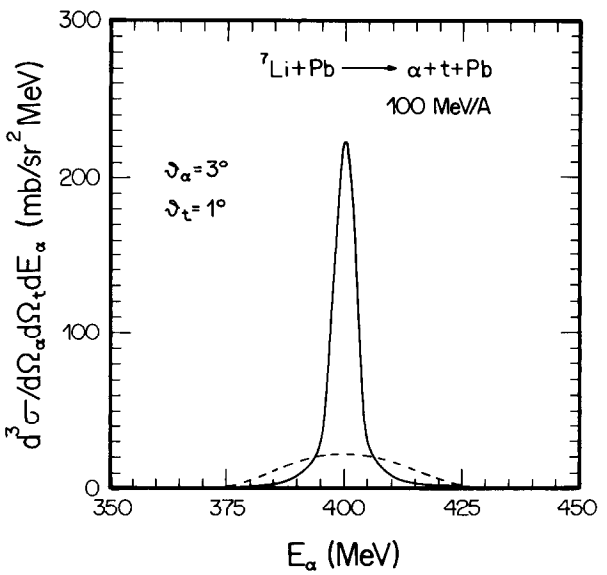

Fig. 6. Triple differential cross section for the break-up of ^{7}Li at 100 MeV/nucleon incident on ^{208}Pb, as a function of the lab energy of the α-particle. The dashed curve results from the nuclear interaction, while the solid one is the contribution from the Coulomb interaction.

TABLE 2

Total cross sections, in mb, for the elastic break-up of loosely bound nuclei incident on ^{208}Pb targets at 100 MeV/nucleon. The Coulomb and nuclear contributions are shown separately and the total cross section includes a (negative) contribution of the Coulomb–nuclear interference

	C	N	Total
^{7}Be	252	12	258
^{16}O	9	52	56
^{7}Li	125	8	131
^{6}Li	11	23	27

of the fragments from the lab measurements. In relation to this, the so-called "magnifying-glass" effect [2]) may be of crucial help to extract precise information about the relative energies.

In any case it seems clear that to have access to the Coulomb matrix elements from break-up reactions, one has to either have a good knowledge of the nuclear contribution to the dissociation, or to look for these situations where the Coulomb interaction is the dominant one. In table 2 we show the total cross sections for the dissociation reactions of eqs. (1a)-(1d), with ^{208}Pb targets and incident energies of 100 MeV/nucleon. The Coulomb and nuclear parts of the total cross sections are given. The sum of the two parts is not equal to the total cross sections due to a small contribution from nuclear-Coulomb interference, which is always negative. The best results are for ^{7}Be and ^{7}Li break-up reactions, in which cases the $L=1$ Coulomb interaction is by far the most effective one.

5. Concluding remarks

Experimental studies of the elastic break-up of loosely bound nuclei have been proposed [2]) as a possible way to investigate the nuclear fusion cross sections of interest in astrophysics. To this aim it is necessary to determine the break-up cross section at low relative energy of the fragments. It is also necessary to disentangle the nuclear and Coulomb interaction effects in the cross sections, as well as the contributions of the different multipolarities to the process. We have shown in this article that, due to its peripheral nature, the nuclear interaction effects may be well accounted for in the "soft spheres" model of Karol, which depends on the nucleon-nucleon scattering amplitudes at the nuclear surface.

A multipole expression of the Coulomb, and nuclear, interaction is straightforward, and is helpful in order to understand the character of the break-up process. In most cases, either the Coulomb or the nuclear $L=1$ terms of the expansion dominate over the $L>1$ terms, largely. This means that, in those cases where the

radiative capture cross section have important participation of high multipolarities ($L>2$), the determination of such contributions from elastic break-up experiments is hopeless. Also, if the nuclear interaction dominates the break-up process, very good experimental strategies have to be found in order to eliminate the nuclear contribution.

The best perspectives occur for clusters with unequal charge-mass ratios, like $\alpha+t$, $\alpha+{}^3He$, etc. In view of the tremendous difficulties to determine the fusion reactions at low relative energies, it is unquestionable that such experiments should be encouraged.

References

1) W.A. Fowler, Rev. Mod. Phys. **56** (1984) 149
2) G. Baur, C.A. Bertulani and H. Rebel, Nucl. Phys. **A458** (1986) 188
3) D.K. Srivastava and H. Rebel, J. of Phys. **G12** (1986) 717
4) C.A. Bertulani and G. Baur, Nucl. Phys. **A480** (1988) 413
5) A.C. Shotter and M.A. Nagarajan, J. of Phys. **G14** (1988) L109
6) D.K. Srivastava, D.N. Basu and H. Rebel, Phys. Rev. **C38** (1988) 2148
7) H. Utsunomiya, R.P. Schmitt, Y.-W. Lui, D.R. Haenni, H. Dejbakhsh, L. Cooke, P. Heimberg and A. Ray, Phys. Lett. **B211** (1988) 24
8) J. Kiener, H.J. Gibs, H. Rebel and G. Baur, Z. Phys. **A332** (1989) 359
9) J. Hesselbarth, S. Khan, T. Kihm and K.T. Knöpfle, Z. Phys. **A331** (1988) 365
10) K. Langanke and S.E. Koonin, Nucl. Phys. **A439** (1985) 384
11) P.J. Karol, Phys. Rev. **C11** (1975) 1203
12) L. Ray, Phys. Rev. **C20** (1979) 1857
13) O. Bernary, L.R. Price and G. Alexander, University of California Radiation Laboratory Report UCRL-20000 NN, 1970
14) C.A. Bertulani, Rev. Bras. Fis. **16** (1986) 380
15) M.S. Hussein, R.A. Rego and C.A. Bertulani, Phys. Reports, in press
16) M.S. Hussein and K.W. McVoy, Nucl. Phys. **A445** (1985) 124
17) M.S. Hussein and R.C. Mastroleo, Nucl. Phys. **A491** (1989) 468
18) C.A. Bertulani and M.S. Hussein, Phys. Rev. Lett. **64** (1990) 1099
19) N. Heide *et al.*, Nucl. Phys. **A504** (1989) 374
20) H. Utsunomiya *et al.*, Nucl. Phys. **A511** (1990) 379
21) G. Baur and M. Weber, Nucl. Phys. **A504** (1989) 352